Supplementary Materials

Naturally Indirect-to-Direct Band Gap Transition in Artificially Fabricated MoS_2 and $MoSe_2$ Flowers

Jun Zhou,[1,#] Juan Cui[2,#], Shuo Du,[3] Zihan Zhao,[4] Jianfeng Guo,[5] Songyang Li,[5] Weifeng Zhang,[4] Nan Liu,[4] Xiaotian Li,[1] Qinghu Bai,[3] Yang Guo,[3], Shuo Mi,[5] Zhihai Cheng,[5] Lin He[1], and J.C. Nie[1], Yang Yu,[2,✉] Ruifen Dou[1,✉]

[1] Department of Physics, Beijing Normal University, Beijing, 100875, P. R. China

[2] LCP, Inst Appl Phys & Computation Math, Beijing 100088, Peoples R China

[3] Beijing National Laboratory for Condensed Matter Physics, Institute of Physics, Chinese Academy of Sciences, Beijing 100190, P. R. China

[4] Beijing Key Laboratory of Energy Conversion and Storage Materials, College of Chemistry, Beijing Normal University, 100875, P. R. China

[5] Department of Physics, Renmin University of China, Beijing 100872, P. R. China

Corresponding Authors:

✉ e-mail: rfdou@bnu.edu.cn;

yang_yu@iapcm.ac.cn;

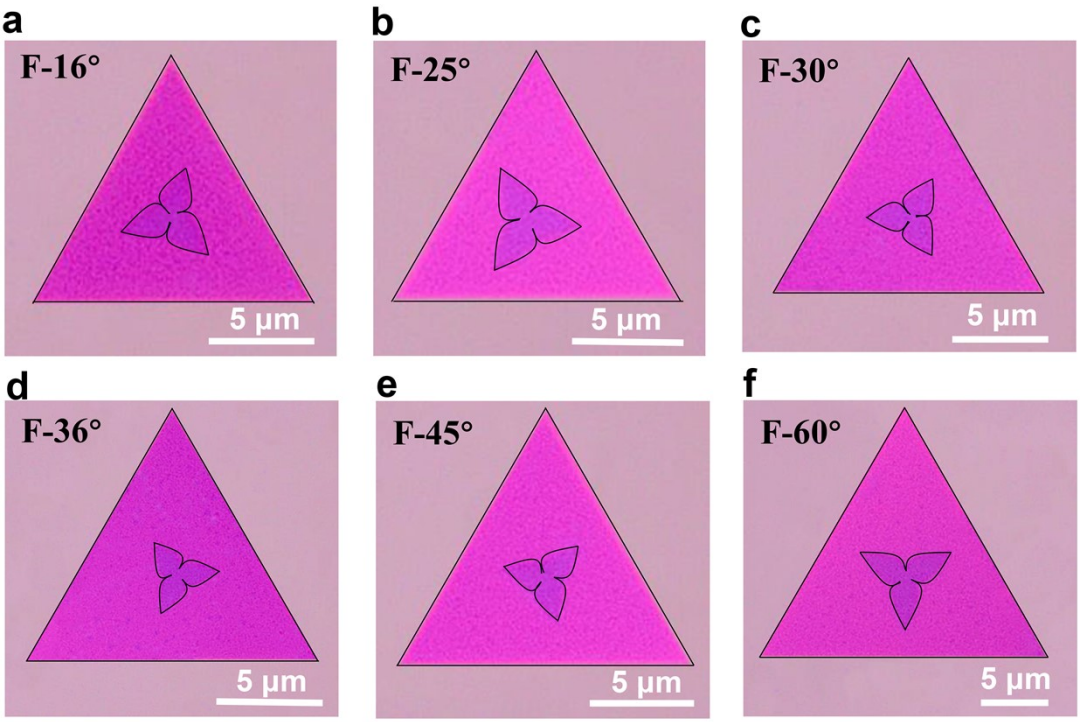

Fig. S1 (a-f) Optical microscopy images of twisted bilayer MoS_2 flower patterns with versatile interlayer twists. The twist is inset in the lift upper corner in (a)-(f).

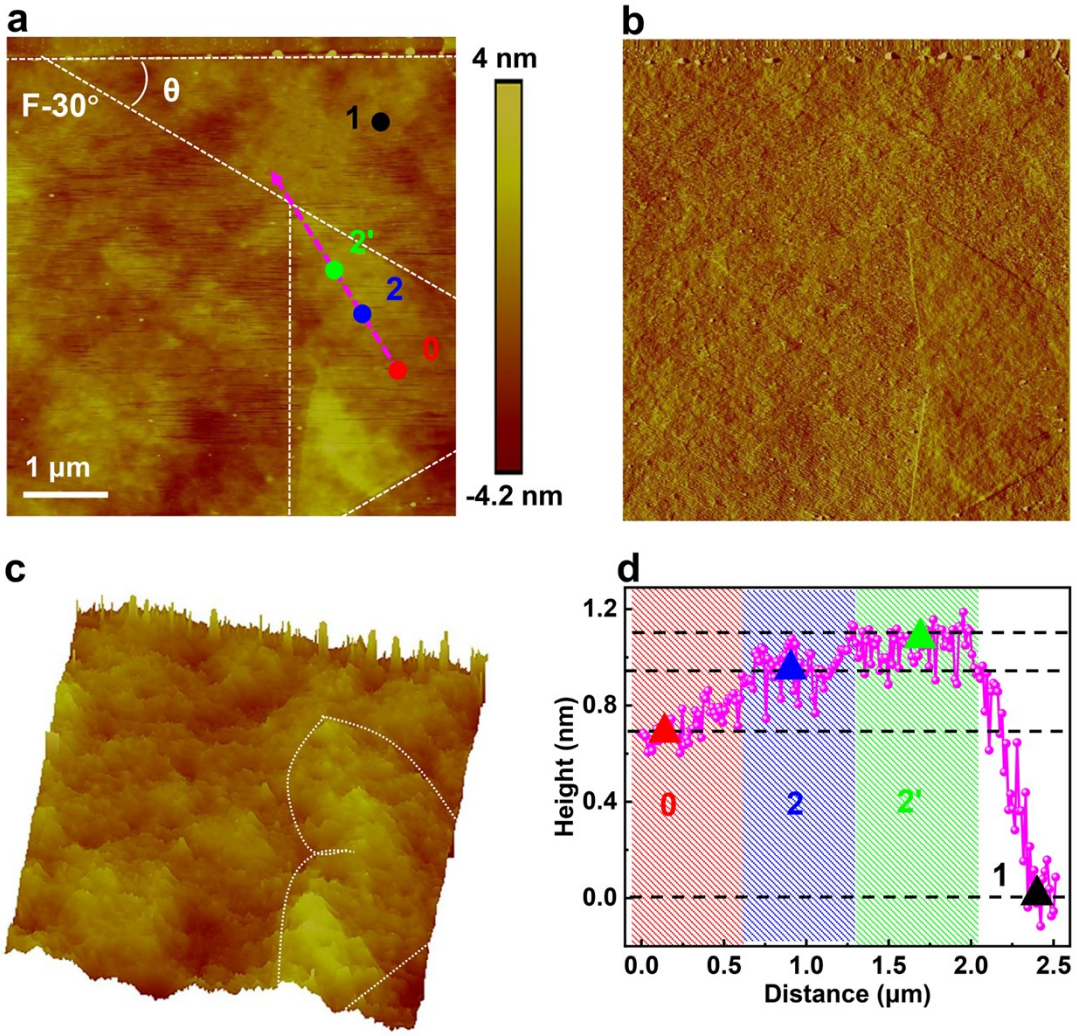

Fig. S2 (a-b) AFM topographic and corresponding phase images of the 30°-tB-MoS_2 flower pattern, respectively. (c) The top flower pattern is zoomed in the right parts of (a) to display the topographic and height difference in 30°-tB-MoS_2 flower. (d) A height profile in (a) marked with pink, showing the changeable interlayer spacing from the center to the off-center region for the 30°-tB-MoS_2 flower.

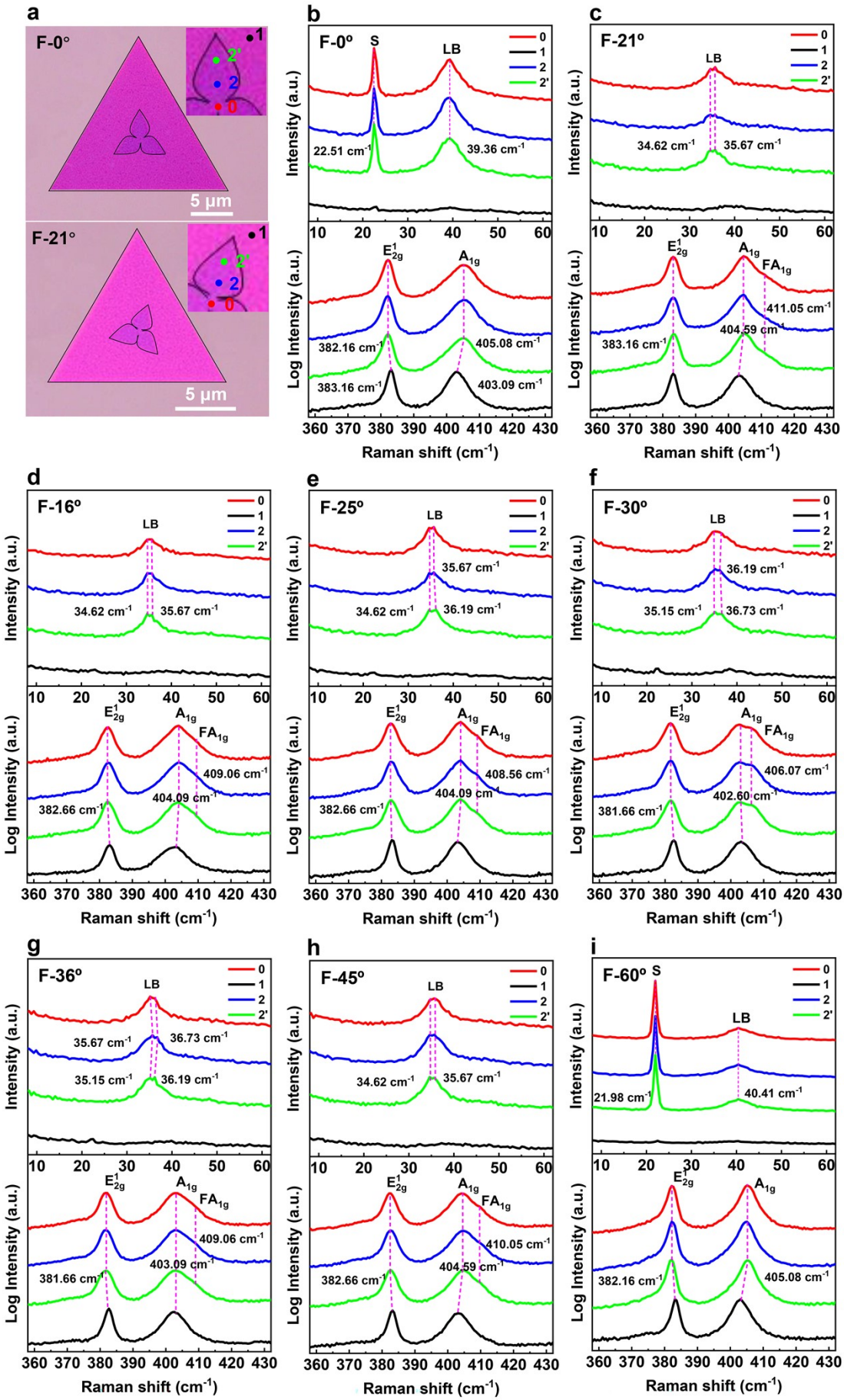
a
F-0°
1
2'
2
0
5 μm
F-21°
1
2'
2
0
5 μm
b
F-0°
S
LB
0
1
2
2'
Intensity (a.u.)
22.51 cm-1
39.36 cm-1
Log Intensity (a.u.)
E12g
A1g
382.16 cm-1
405.08 cm-1
383.16 cm-1
403.09 cm-1
Raman shift (cm-1)
c
F-21°
LB
34.62 cm-1
35.67 cm-1
FA1g
411.05 cm-1
404.59 cm-1
383.16 cm-1
d
F-16°
34.62 cm-1
35.67 cm-1
409.06 cm-1
404.09 cm-1
382.66 cm-1
e
F-25°
35.67 cm-1
34.62 cm-1
36.19 cm-1
408.56 cm-1
404.09 cm-1
382.66 cm-1
f
F-30°
36.19 cm-1
35.15 cm-1
36.73 cm-1
406.07 cm-1
402.60 cm-1
381.66 cm-1
g
F-36°
35.67 cm-1
36.73 cm-1
35.15 cm-1
36.19 cm-1
409.06 cm-1
403.09 cm-1
381.66 cm-1
h
F-45°
34.62 cm-1
35.67 cm-1
410.05 cm-1
404.59 cm-1
382.66 cm-1
i
F-60°
S
LB
21.98 cm-1
40.41 cm-1
382.16 cm-1
405.08 cm-1

Fig. S3 (a) Optical microscopy images of 0°- and 21°-tB MoS_2 flower patterns with a highlighted area showing different Raman detection regions (**0**, **2**, **2'**, and **1).** (b-i) LF and HF Raman spectra obtained from the tB-MoS_2 flower patterns with a twist angle of 0°, 16°, 21°, 25°, 30°, 36°, 45°, and 60°, respectively. Four different colored Raman curves from (b) to (i) are from the region **0**, **2**, **2'**, and **1**.

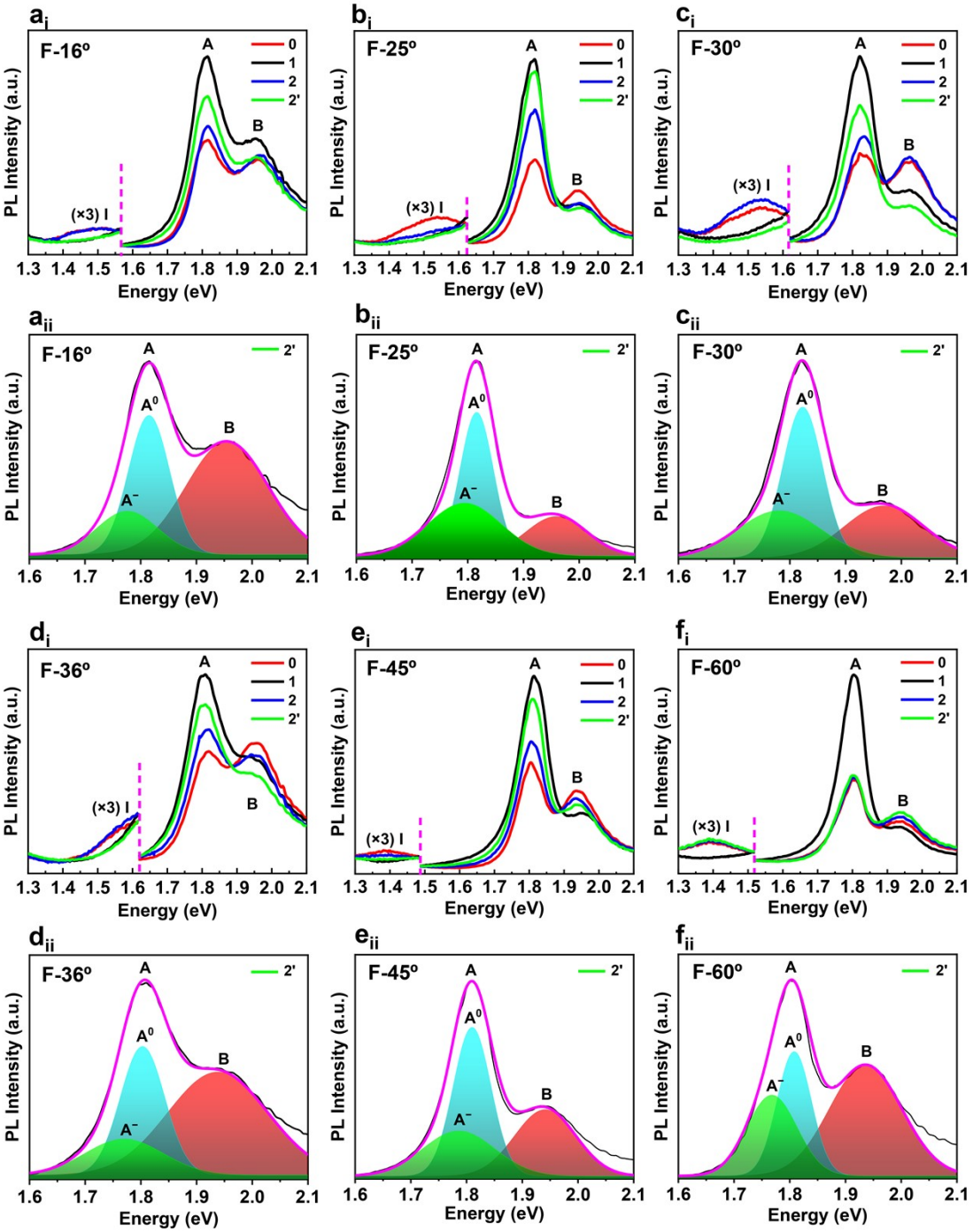

Fig. S4. (a_i-f_i) PL spectrum acquired from samples of tB-MoS_2 flower patterns with a twist of 16°, 25°, 30°, 36°, 45° and 60°, respectively. Four different colored curves including the red, the blue, the green and the black curve from (a_i) to (f_i) are obtained from the region **0**, **2**, **2'**, and **1** in the above samples. (a_{ii}-f_{ii}) Deconvoluted PL spectrum from the region **2'** corresponding to (a_i)-(f_i), respectively.

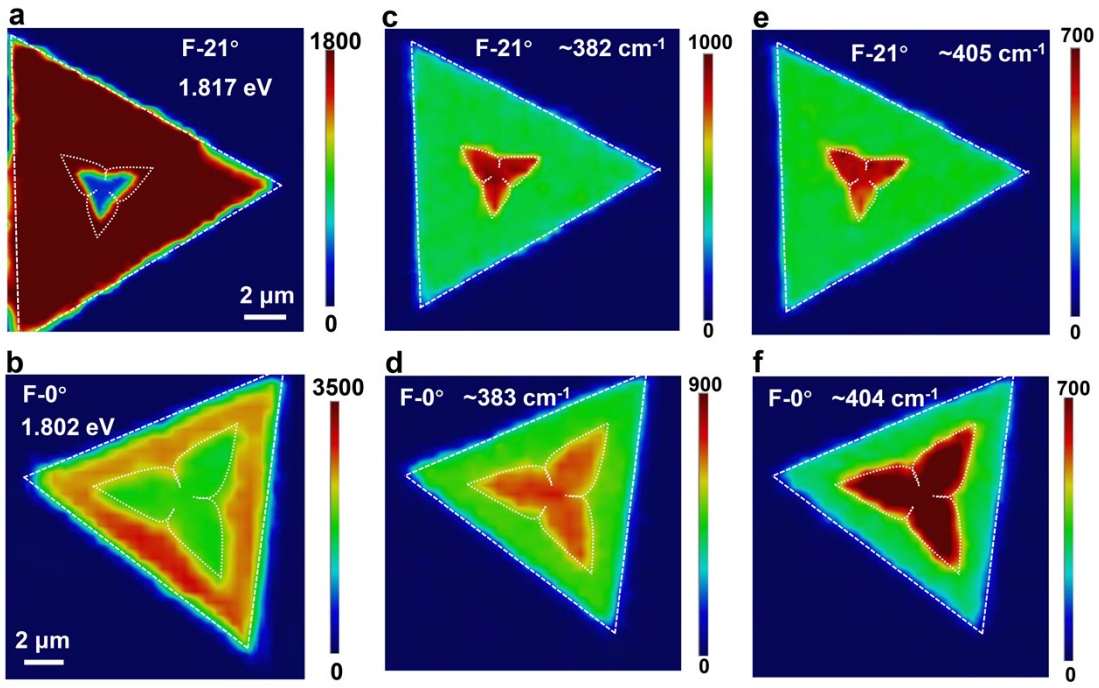

Fig. S5 (a, b) PL intensity mapping images of the 21°-tB-MoS_2 and 0°-tB-MoS_2 flower patterns obtained at the energy of A exciton peak positions of 1.817 and 1.802 eV, respectively. (c, d) Raman intensity mapping images of the 21°-tB-MoS_2 and 0°-tB-MoS_2 flower patterns for the E^1_{2g} and A_{1g} modes, respectively.

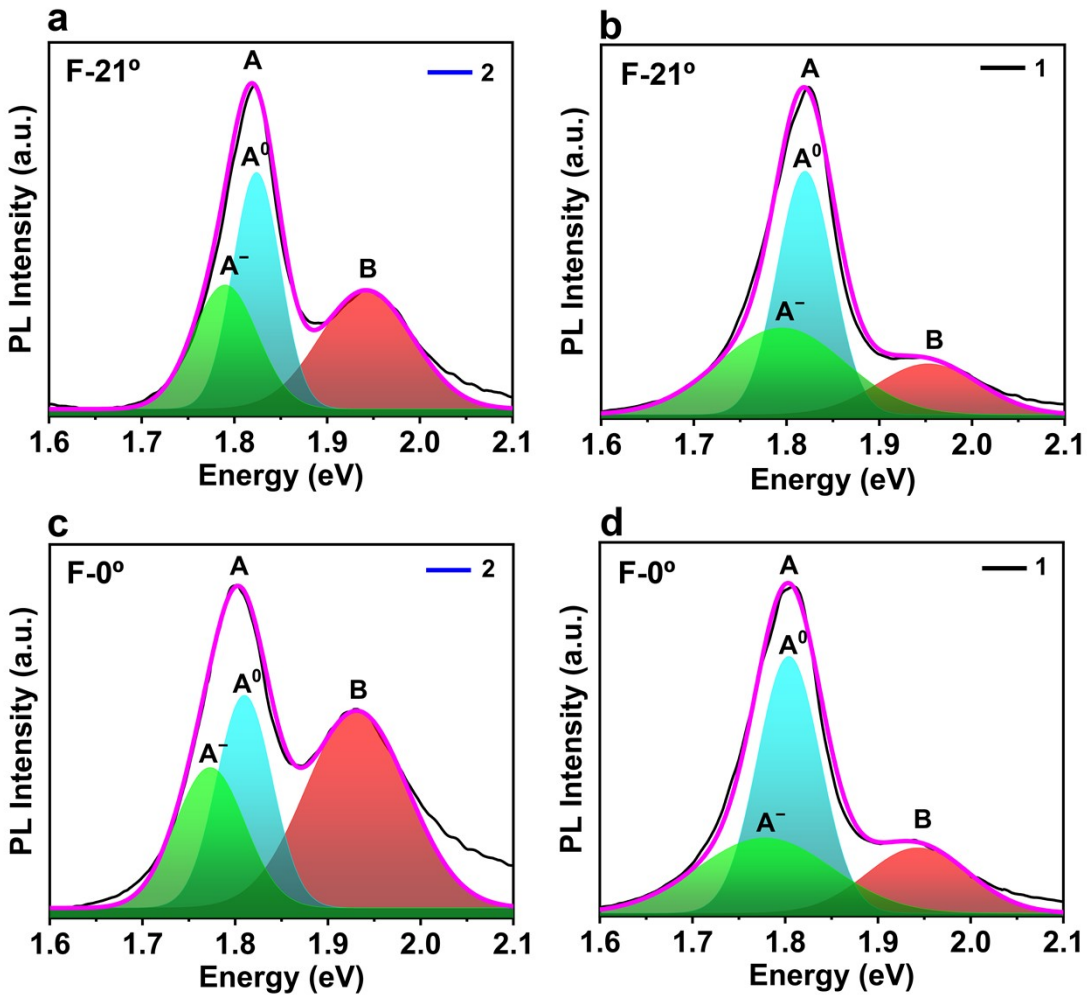

Fig. S6 (a, b) Deconvoluted PL spectrum from the region **2** and **1** from 21°-tB-MoS_2 flower pattern, respectively. (c, d) Deconvoluted PL spectrum from the region **2** and **1** from 0°-tB-MoS_2 flower pattern, respectively.

Table I. Calculated interlayer spacing Δd (nm), effective masses (in unit of free electron mass m_o) at **K** for bilayer MoS_2 flower pattern with different twisted angles.

Twisted angle	Region	Δd (nm)	CBM-m_e (m_0)	VBM-m_h (m_0)	Bandgap
21°	0	0.63	0.5/0.99906=0.500	0.5/0.82925=0.603	Indirect
21°	2	0.75	0.5/1.00217=0.499	0.5/0.83202=0.601	Indirect
21°	2'	0.95	0.5/1.00193=0.499	0.5/0.83634=0.598	Direct
21°	1		0.5/0.97886=0.511	0.5/0.80988=0.6174	Direct
0°	0	0.60	0.5/0.83763=0.597	0.5/0.7939=0.63	Indirect
0°	2	0.60	0.5/0.83763=0.597	0.5/0.7939=0.63	Indirect
0°	2'	0.60	0.5/0.83763=0.597	0.5/0.7939=0.63	Indirect
0°	1		0.5/0.97886=0.511	0.5/0.80988=0.6174	Direct

DFT Calculations

DFT calculations were performed using the Vienna *ab initio* simulation package (VASP) [1]. The Perdew-Burke-Ernzerhof (PBE) generalized gradient approximation[2] and the projector-augmented wave method[3] were employed to describe the exchange correlation energy and the electron-ion interaction, respectively. We adopted a plane wave cutoff energy of 400 eV and a convergence criterion of 10^{-5} eV in all calculations. In the self-consistent calculation, a *k*-point mesh density of $2\pi\times$ 0.03 $Å^{-1}$ using the **Γ**-centered Monkhorst-Pack scheme[4] was adopted. The vacuum thickness was set large enough (>30 Å) in the z-direction to avoid interactions between periodic sheets of tB-MoS_2. In our calculations, van der Waals interactions were considered under the framework of the vdW-DF method with the optB86b-vdW exchange functional[5]. To study the electronic band structures of twisted-bilayer MoS_2 (tB-MoS_2), we calculated the effective band structures of the crystallographic superlattice using the band unfolding technique[6].

In this study, the strain in 21°-tB-MoS_2 flower caused the interlayer spacing difference between the center region **0** and the edge region **2'**, which was not observed in 0°-tB-MoS_2 flower. Therefore, we constructed a crystallographic superlattice unit cell of the tB-MoS_2 with θ=21.79° and various layer distance (Δd). The size of each petal of the flower pattern was about 2.5 μm and the region we simulated is at the scale of ~1 nm, which could be regarded as a point of the petal, as depicted in **Fig. S**7. The interlayer distance Δd was set as 0.63 nm to simulate the atomic structure at the center region **0**. We increased the Δd to 0.70nm, 0.75nm, and 0.80 nm to simulate the atomic structure at the edge region **2'**, the energy band structures of which are shown in **Fig. S**8. We can see that the energy band structure transition from the indirect gap to the direct one with the interlayer spacing increasing up to 0.75 nm. In our case, the experimental measured interlayer spacing in region 2 for the sample of 21°-tB-MoS_2 is enlarged to around 0.95 nm. Therefore, it is rational to observe the energy band gap transition.

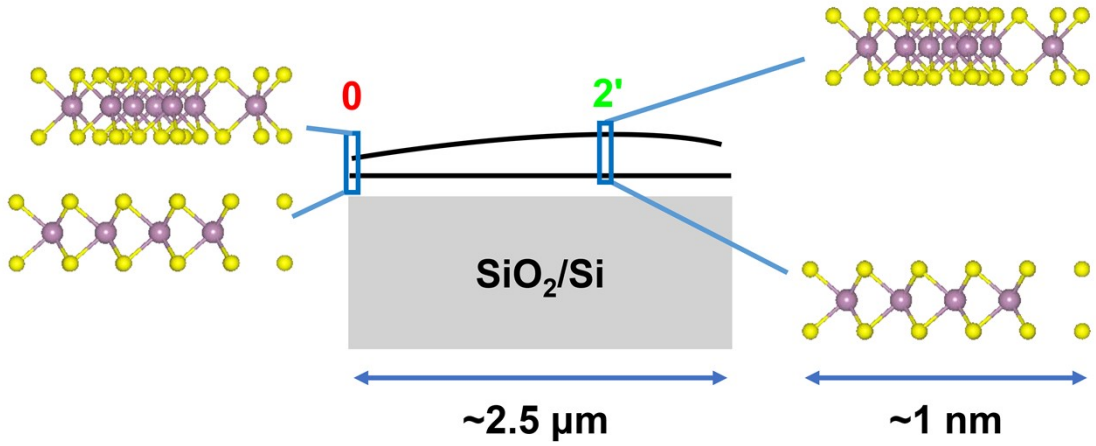

Fig. S7 Theoretical model for the twisted bilayer MoS_2 with θ=21.7° at different regions.

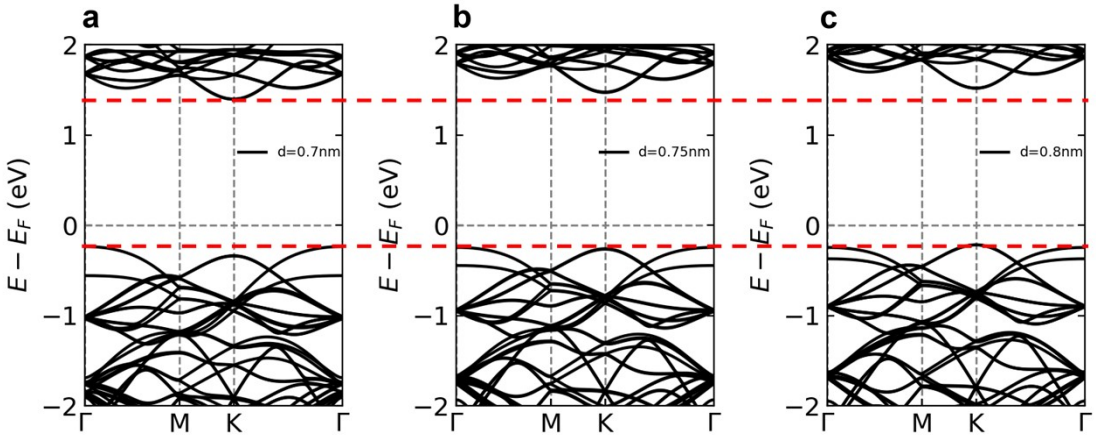

Fig. S8 The energy band structures of the twisted bilayer MoS_2 with θ=21.79° with different interlayer distances.

Additional References

1. G. Kresse and J. Furthmuller, *Phy. Rev. B*, 1996, **54**, 11169-11186.
2. J. P. Perdew, K. Burke and M. Ernzerhof, *Phys. Rev. Lett.*, 1996, **77**, 3865-3868.
3. P. E. Blochl, *Phy. Rev. B*, 1994, **50**, 17953-17979.
4. H. J. Monkhorst and J. D. Pack, *Phy. Rev. B*, 1976, **13**, 5188-5192.
5. J. Klimes, D. R. Bowler and A. Michaelides, *Phy. Rev. B*, 2011, **83**, 195131.
6. V. Popescu and A. Zunger, *Phy. Rev. B*, 2012, **85**, 085201.